[AV]Enhanced Monitoring of Geologic Carbon Sequestration Using 3-D Passive Microseismic Location Techniques

Delaine Reiter[1] and William Rodi[2]

Search and Discovery Article #110088 (2009)
Posted July 25, 2009

*Adapted from oral presentation at AAPG Annual Convention, Denver, Colorado, June 7-10, 2009

[1]Weston Geophysical Corp., Lexington, MA (delaine@westongeophysical.com)
[2]Massachusetts Institute of Technology, Cambridge, MA.

Abstract

In recent years there has been a significant increase of interest in real-time passive monitoring of microseismicity related to carbon dioxide sequestration in geological formations. We have adapted a sophisticated 3-D location algorithm originally designed for regional and teleseismic applications to microseismic monitoring of shallow underground reservoirs. Our technique has many features that are of significant value to small-scale applications, such as the accommodation of down-hole stations, the use of azimuth data in addition to arrival times, travel-time forward modeling with 3-D velocity models, and the computation of 3-D confidence regions on the calculated hypocenters. In addition to modifying the location algorithm, we also developed a wavelet-based phase detection algorithm to accurately pick microseismic P and S arrival times and a polarization algorithm to determine the arrival azimuths of P waves. To date we have applied the microseismic version of our location algorithm to two data sets, including a field study of hydraulic fracturing following fluid injection at a site in southeast Texas and a synthetic study using the geometry from a small-scale carbon injection pilot site. The results from both case studies demonstrate that we can accurately locate and characterize microseismicity in a realistic 3-D velocity model using both arrival times and azimuths measured by a sparse network of downhole sensors.

Enhanced Monitoring of Geologic Carbon Sequestration Using Three-Dimensional Passive Microseismic Location Techniques

Delaine Reiter and William Rodi

AAPG Annual Meeting, Denver, Colorado
June 9, 2009

CO_2 Sequestration Monitoring Scenario

- Variety of geologic storage environments
- Storage injection rates much lower than typical hydrofrac
- Stand-off passive monitoring distance similar to hydrofrac (but the closer the better)
- Designed to keep induced seismicity low

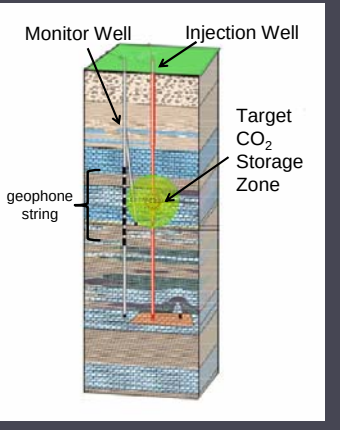

Presenter's Notes: Many of you are familiar with the planned carbon dioxide (CO_2) sequestration projects that are ramping up across the US and even overseas. The basic idea of geologic sequestration is to inject CO_2 into underground formations and hold it there indefinitely, thereby addressing (hopefully) climate change in a large-scale way.

There are a variety of geologic carbon storage environments that are being tested right now, including depleted oil and gas reservoirs, enhanced oil recovery operations, deep unused saline aquifer reservoirs, and unminable coal seams, for example. In most of these storage environments the injection rates are going to be held fairly low, to prevent the escape of the injected CO_2 –as low as 1/10 of the rates that typical hydrofrac experiments use. The cartoon on the right represents what will typically be the passive seismic monitoring setup for a CO_2 injection scenario. The setup will usually include only one monitoring well with geophones spaced to cover the injection zone, at a standoff distance that's similar to a hydrofrac (on the order of 500-1500'). The closer we can get to the injector, the better, since the seismicity induced by lower injection rates is almost certainly going to be lower than that in a more typical Enhanced Oil Recovery (EOR) environment. It is designed this way because keeping the induced seismicity low helps the field operators ensure that the storage reservoir is well sealed.

In our work we want to accurately locate any microseismicity that is induced during a CO_2 injection, and having a sophisticated location algorithm is an important part of that effort. While we will be working on the scenario in which you hope *not* to induce seismicity, we are testing and refining our techniques in the hydrofrac monitoring world, which has a lot of overlap in geometry and geologic background, but with much more abundant seismicity to practice on.

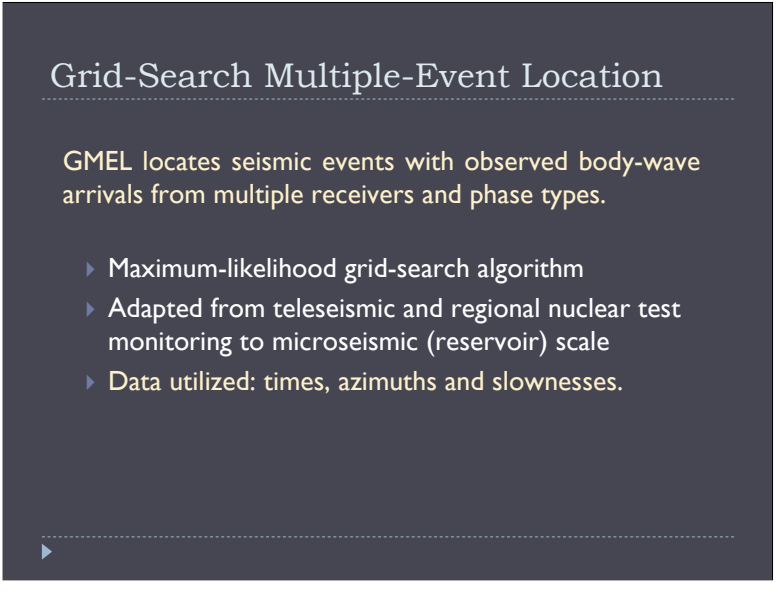

Presenter's Notes: Our location algorithm is known as the grid-search multiple-event location technique (GMEL). GMEL is a seismic event locator that uses measurements from body-wave arrivals (most typically P and S first arrivals) at multiple receivers (including those on the surface or in the borehole or any combination) to produce an estimate of hypocenter (location in space and origin time).

Like many modern event location techniques, it uses the mathematics of maximum likelihood to calculate the best-fitting hypocenter after a nested grid-search over increasingly fine regions of potential hypocenter locations.

GMEL was originally developed by Dr. Bill Rodi at MIT to address the difficult problem of accurately locating events that are sparsely observed at regional and/or teleseismic distances – events that could be nuclear explosions conducted in a clandestine manner. Weston partnered with Dr. Rodi to develop better travel-time prediction capabilities in GMEL so that we could overcome the biases in the event locations caused by using incorrect or over-simplified velocity models.

Over the years GMEL has become increasingly sophisticated in its abilities to incorporate a variety of data types such as times, azimuths and arrival slownesses that can be found from applying beam-forming techniques to different types of arrays including those on the Earth's surface or the linear arrays found in the borehole.

So far what I have described might not be too exciting to many of you – most of the currently available location algorithms have at least a portion of the capabilities I'm describing. In the next couple of slides I hope to convince you that GMEL has additional capabilities may yield a better understanding of reservoir microseismicity.

GMEL Travel-Time Prediction

- Time predictions from homogeneous up to 3-D velocity models
- Ray tracing with choice of two different algorithms:
  - Finite-difference first arrival
  - Ray bending

Example Regional 3D P Ray Path

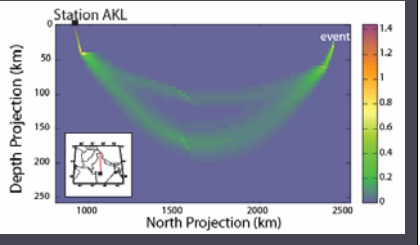

Presenter's Notes: One unique capability of GMEL is in the travel-time prediction component of the location. As computer speed and capacity have grown, the ability to represent more realistic subsurface velocities has also gotten better. GMEL can utilize travel-time tables from flat background models (0D) up to fully 3D models. It also has two types of 3D travel-time modeling available depending on the application, including a finite-difference technique for first arrivals and a ray bending technique that can do first as well as later arrivals. We find that the finite-difference algorithm works better for the reservoir-scale problem, since it finds arrivals even in shadow zones caused by low velocity layers.

To demonstrate the finite-difference algorithm, the figure on the right shows the ray path sensitivities found with the finite difference technique along a regional path between a station and event in India. This example shows that the minimum-time path between event and receiver actually samples a large depth interval in the upper mantle, rather than following a simple geometrical path just beneath the crust-mantle discontinuity. At the reservoir scale the raypaths do not appear to behave quite so strangely, but we have not examined many cases yet.

Location Error Analysis

- The standard methodology calculates a confidence *ellipsoid* on an event hypocenter based on simplifying assumptions:
  - Travel time (and azimuth, a-o-i) is a *linear* function of the event hypocentral location
  - Data errors obey a Gaussian distribution
- With these assumptions, the ellipsoid parameters (axis lengths, orientation) can be found with analytic formulas.

With sparse coverage and poor aperture, the linearity assumption is particularly questionable

Presenter's Notes: A real advantage to GMEL is its approach to error analysis, which differs from the standard analysis typically done. In an nutshell, the standard methodology calculates the confidence on a location as an ellipsoid that is derived using two assumptions. The first is that the travel time, as well as the azimuth and angle of incidence, is a linear function of the hypocenter location. The second is that data errors obey a Gaussian distribution. When you make these assumptions you get analytical formulas that are used to calculate ellipsoid parameters at a certain confidence level, for example 90%.

Unfortunately, when you are computing a location from observations that are sparse or have poor aperture surrounding the event from different azimuths, you are not obeying the assumptions governing standard error ellipsoids. This can cause a big underestimation of the actual errors on the event location.

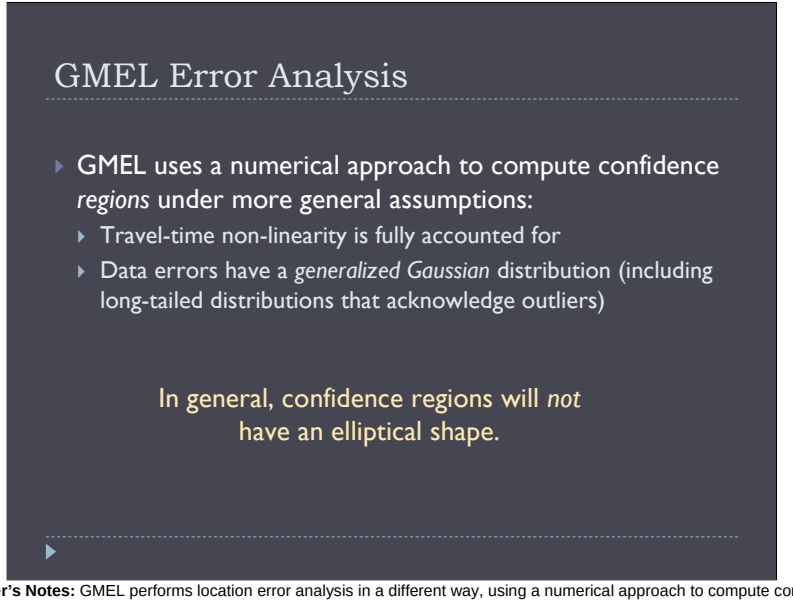

Presenter's Notes: GMEL performs location error analysis in a different way, using a numerical approach to compute confidence regions that incorporate more general assumptions. In the numerical approach the nonlinear behavior of the travel times is fully accounted for. And the data errors are no longer required to obey a standard Gaussian distribution – they are generalized to include some of the typical distributions that we see in the location procedure such as bimodal distributions or outliers.

The numerical approach definitely adds to the computation burden compared to the standard analytical solution. However, when we apply this type of numerical error analysis to poorly constrained location applications, we find that the confidence regions can take on very unusual shapes that are rarely elliptical in shape.

Reservoir-Scale Simulation

Two sets of events:

1. Narrow band in injection interval
2. Diffuse cluster below injection interval

One observation well:

Seven geophones spaced at 15-m intervals; stand-off distance 426m (~1400')

Velocity model:

1-D P and S smoothed from sonic logs

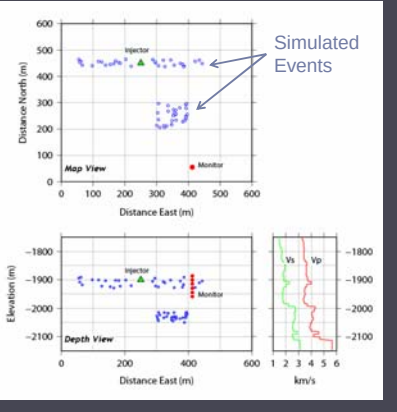

Presenter's Notes: To illustrate some of these concepts I simulated a scenario in which there is a single injection well at a particular depth zone with a single observation well at a distance from the injector of 426 m. The monitoring tool string is small, with only seven three-component geophones spaced at 15-m intervals near the depth of the injector.

To orient you to the plots we will be seeing in the next slides: the top subplot shows a map view of the true locations of some microseismic events (blue circles); the bottom left subplot shows a depth view of those events. The injector well position is shown as a green triangle and the monitor well geophone string is indicated with red circles. On the bottom right is a small plot of the P (compressional wave) and S (shear wave) velocity models we used to predict our travel-time observations.

Next we generated two clusters of events to relocate. One cluster is a narrow band of events occurring in the injection interval, and the other is a diffuse cluster occurring beneath the injection interval in a higher velocity zone.

Synthetic Simulation Data

- Finite-difference travel times from 'true' velocity model
- Straight flight-path azimuths
- Contaminated with noise:

Phase Type	Time Std Dev	Azim Std Dev
P	2.0 ms	6 °
S	4.0 ms	8 °

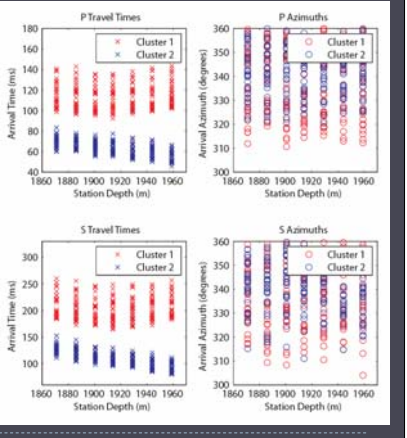

Presenter's Notes: We used our first-arrival finite-difference algorithm to generate a suite of travel times from the true event positions to the seven geophones using the layered velocity models shown in the previous slide. We also generated azimuth data from the straight path angles between the events and stations. Then we contaminated all of the data using noise with the standard deviations shown in the table on the bottom left. The noisy P data had a standard deviation of 2 ms on the travel times and 6 degrees on the azimuths. The noisy S data had a larger standard deviation of 4 ms on the travel times and 8 degrees on the azimuths. On the right I show a plot of the noisy times and azimuths for both P and S data and both clusters of events.

These are the data we invert with GMEL, looking to see how well the events located with noisy data compare with the true locations. We will first look at the results when we include only the P and S time data from all the stations. I note that we make the assumption that some brilliant analyst has already associated the correct travel-time picks with individual events – bypassing a whole other data processing problem in the location procedure that must be dealt with – only not during this talk.

Locations: P & S Times Only

- Lateral and depth movements allowed up to 100m, time up to 10ms
- True velocity model and all stations used in relocations

Aperture of the array is so narrow that time data cannot constrain the locations.

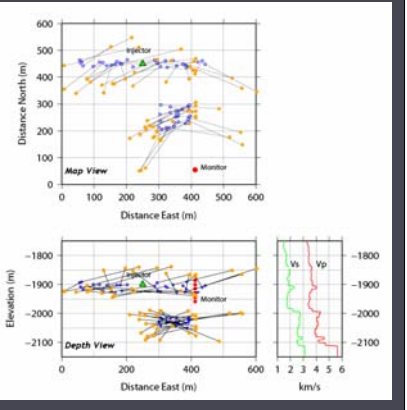

Presenter's Notes: This slide shows the results when we use GMEL to relocate the events with noisy P and S travel-time data from all the geophones. We gave GMEL some help by letting the lateral and depth movements of an event shift up to 100 m and the origin time of the events up to 10 ms from the true event position. In other words we gave GMEL a limited range and depth interval in which to find the event positions - thereby providing information we wouldn't have in a field experiment. In the map and depth view to the right the orange circles show the locations that GMEL finds that best fit the travel time data. There are lines drawn between the true locations and the final GMEL locations.

As you might expect, the locations are terrible, many of them moving the maximum allowable distance either laterally or in depth. The aperture of the array is so narrow that time data alone are not able to constrain the locations.

Locations: P & S Times And Azimuths

All P & S azimuth data included (unrealistic in field data)

Locations are better constrained in general, but split into bands

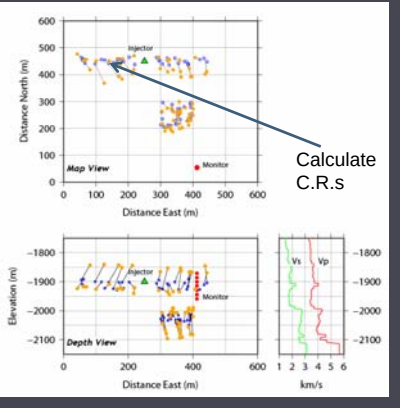

Presenter's Notes: Next we performed a more reasonable estimate of the locations in which we added the P and S azimuth data to the travel- time data. This results in total of 28 data points to use in each event location (7 P times, 7 S times, 7 P azimuths and 7 S azimuths). I note that this is not a realistic scenario with field data, since it is rare to have such a clean data set that you can perform analysis on every data trace and get good travel-time and azimuth estimates for all events and all stations. However, I included them here to help clearly illustrate my points.

We use GMEL to invert the data for new event locations, using the same constraints as in the previous example (including travel-time predictions from the correct velocity model). The results to the right show that the locations in general are much better constrained, but appear to break into narrow bands in depth. This might tempt an analyst into over-interpreting the presence of fractures or other subsurface features. To prevent that, we can use the calculation of numerical confidence regions to look into the behavior of a specific event in Cluster 1 shown by the arrow.

Error Analysis: P & S Times And Azimuths

Cluster 1 event moved to the SE by 57 m and up to top of location grid 66 m above.

90% C.R. indicates equal confidence in a narrow 'boot' shape that covers a large subsurface volume.

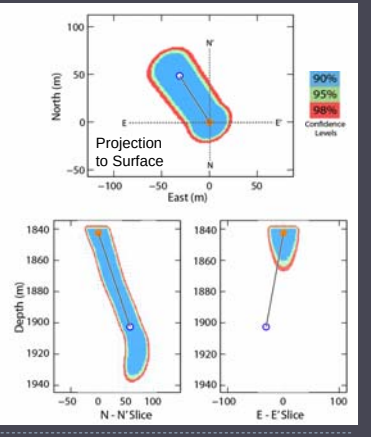

Presenter's Notes: When we zoom in on the event and plot the confidence regions, we can see some unusual features. Currently we display the 3D confidence regions computed by GMEL in a less than ideal manner. In the top subplot I show a projection to the surface of the confidence region at depth. The 'ground truth' for the event (i.e. the true location) is shown as a blue circle, and the final location computed by GMEL as a orange circle. The two plots on the bottom show the slices along the N-N' and E-E' dotted lines in the top plots. There are some mental gyrations required to visualize the results in 3D hypocenter space, but the basic shape of location confidence is clearly not ellipsoidal in nature.

The location results show that GMEL computed the event to be 66 m shallower and 57 m to SE compared to its true position. The confidence regions show that there is 90% confidence that the event took place in a narrow boot-like shape that extends over 80 m in depth and approximately 30 m in lateral extent surrounding the GMEL event position. In this case the 90% confidence region does encompass the true position, although this is frequently not the case. Some of the other cluster event relocations do not produce such strongly non-elliptical confidence regions, but this type of result is typical.

Locations: Tool Aperture Doubled

Double the spacing between each geophone and include all times and azimuths

Locations are better constrained in depth and epicenter

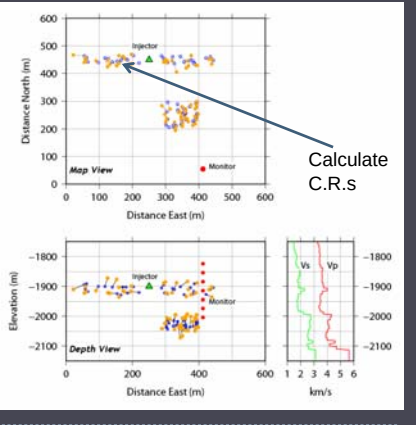

Presenter's Notes: We can look at experiment design with GMEL, for example, by varying the spacing of the geophones along the tool string. If we take the original seven geophones and use 30-m spacing in depth as opposed to 15 m, we get better constrained locations in both depth and epicenter for both simulated clusters. Again, this is a best case scenario, because we still used all the P and S data, both times and azimuths, to achieve these results. In a field setting, you might risk missing some detections of the smallest (or farthest away) events on the geophones that are at the bottom or top of the tool string. However, there are significant benefits to increasing the aperture of your observations in the situation where you only have one monitor well.

We can again take the same event as in the previous example and calculate the confidence regions for comparison.

Error Analysis: Doubled Tool Aperture

Cluster 1 event moved to the NW by 18 m and up 23 m in depth.

90% C.R. indicates a more regular ellipsoid shape elongated along angle between event and geophone array.

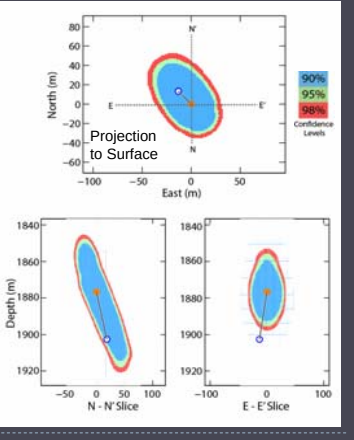

Presenter's Notes: Here we display the same type of results as in the previous example, but the experiment aperture has been doubled. The location results for the same event now move to the NW by 18 m (less than a 1/3 of the distance in the previous example) and again shallower in depth by 23 m (about half of the previous amount).

The confidence region results look much more 'normal', with a more regular ellipsoidal shape. The location is still less well constrained than the standard analysis would show; it is also not that well constrained along the angle between the event and the geophone array.

Locations: Simplified Velocity Model

Invert using simple gradient velocity model, larger tool aperture and all data

Locations shift systematically depending on distance from tool string

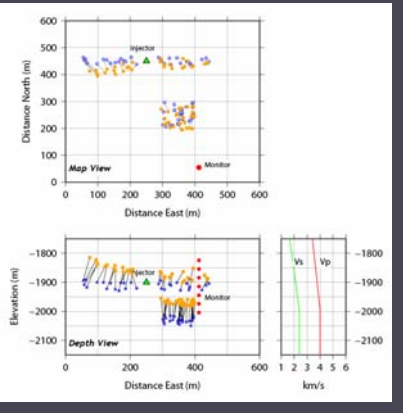

Presenter's Notes: As a final example of GMEL analysis, I also located the noisy simulated data (both times and azimuths) using the same constraints as before, but with travel-time predictions that were generated from a simple gradient over a half-space model shown in the plot on the lower right. We also retained the doubled aperture of the experiment to take advantage of the better network geometry. In this case we can use very simple 1-D ray tracing methods to compute the predicted travel times.

The results show that the locations are relatively good, although the shift in the lower cluster in depth brings those events much closer to the depth of events in Cluster 1. Overall the event locations shift systematically depending on their distance from the geophone string.

Comments

- Error analysis should be considered a key component of any microseismic mapping exercise
  - Without it the locations should be considered speculative
- Designs of passive monitoring experiments should always include maximizing aperture (coverage) and careful velocity modeling

Presenter's Notes: In summary, I first note that the simple simulated scenarios we showed in this talk indicate that there is need for careful error analysis in reservoir scale locations. It may not be the glamorous part of the whole process, but it is critical to understanding the potential event movements you might see in a field setting. If there is no error analysis attached to the mapping of microseismicity, the locations should be considered incomplete and highly speculative. That's a bold statement, but there's no getting around the truth of it.

Second, the design of the experiment should be carefully considered before deployment. It's important to look at geophone spacing or ideally adding another monitor well with even a single geophone to help constrain the locations better. Finally, velocity modeling is a big issue that I didn't discuss extensively, but experimenting with different velocity models built from different sources (e.g. sonic logs or string shots) is an important step in getting the best locations.

Application to Field Data

- Weston is a participant in SECARB Phase II Field Test 1 in an Enhanced Oil Recovery setting ahead of large scale brine injection down-dip of EOR.
- CO2 flood will be monitored for sweep efficiency and seal effectiveness.

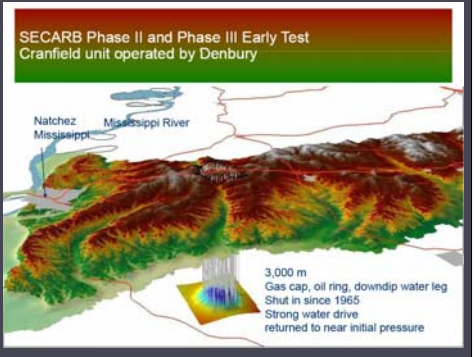

Presenter's Notes: In terms of field applications outside of the simulations I have shown here, Weston is scheduled to test our passive monitoring capabilities using the data from a planned CO_2 storage process in an active oil field. We are participating in a DOE-sponsored field test through the southeast regional carbon sequestration partnership (or SECARB). We are specifically part of a Phase II field test at a site near Cranfield, MS, in a unit operated by Denbury Resources, Inc.

The field test is going to be in an enhanced oil recovery (EOR) setting that will use CO_2 as the injection flood. We will be doing this field test ahead of a full-scale CO_2 injection in a saline aquifer that is down dip of the EOR test. The CO_2 flood we will be monitoring is primarily focused on determining the sweep efficiency and seal effectiveness at the Cranfield site.

Passive Monitoring Field Application

- Single monitoring well with 515' total aperture that will straddle the injection zone
- Weston will process 3 months of continuous microseismic data with GMEL and other software to locate and characterize any induced seismicity.

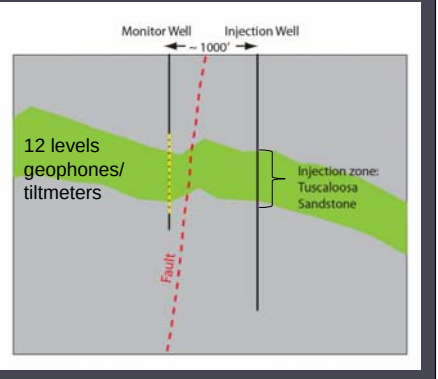

Presenter's Notes: This slide shows a cartoon mockup of what is being called the 'geomechanical test' that Weston is involved in. The injector and monitor wells are on opposite sides of a fault, which is closer to the monitor well. The injection interval is in the lower Tuscaloosa Sandstone, and a single monitoring well is approximately 1000' away. We plan to passively monitor three months of the injection using a 12-geophone and tilt meter tool deployed by Pinnacle Technologies. We will process the continuous microseismic data using GMEL and other software to locate and characterize any induced seismicity that occurs.

Acknowledgements

- Funded under DOE Small Business Innovative Research Grant # DE-FG02-07ER84683
- UT Austin Bureau of Economic Geology (Tip Meckel, Susan Hovorka), Lawrence Berkeley National Lab (Jonathan Ajo-Franklin)